Near-infrared luminescence and magnetic properties of dinuclear rare earth complexes modulated by *β*-diketone Co-ligand

Ling Li,[a] Jian Gou,[a] Dong-Fang Wu,[a] Yun-Juan Wang,[a] Yao-Yao Duan,[a] Huan-Huan Chen,[a] Hong-Ling Gao*[a,b] and Jian-Zhong Cui*[a,b]

List of contents

Section S1 Supplementary Experimental Section

Section S2 Powder X-ray Diffraction, UV-Vis spectra, Thermogravimetric Analysis and Near-infrared luminescence spectra

Section S3 Plots of Magnetic Data

Section S4 Crystallographic Data and Continuous Shape Measures Values

[a]*Department of Chemistry, Tianjin University, Tianjin, 300354, China.*
** Corresponding authors, E-mail: cuijianzhong@tju.edu.cn, ghl@tju.edu.cn.*
[b]*Key Laboratory of Advanced Energy Materials Chemistry (Ministry of Education), Nankai University, Tianjin, 300071, China.*

Section S1 Supplementary Experimental Section

Scheme S1 The synthesis of 3-methoxysalicylaldehyde-2-aminobenzoylhydrazone (H_2L).

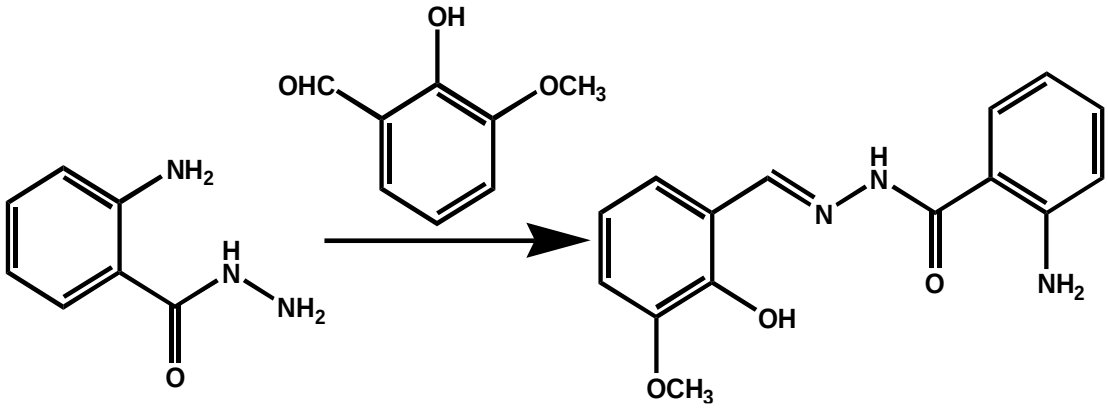

To a solution of 2-hydroxy-3-methoxybenzaldehyde (10 mmol) in methanol was added a solution of 2-aminobenzhydrazide (10 mmol) in methanol (Scheme S1). The reaction mixture is stirred four hours at room temperature, a crude product was obtained, which was washed with methanol and dried in vacuo to give the H_2L ligand as a milky solid. The milky precipitate was heated to reflux in methanol and recrystallized to give a pale crystalline solid. Yield: *ca*. 85%. Elemental analysis (%), calcd for $C_{15}H_{15}N_3O_3$ (fw = 285.29): C, 63.15; H, 5.30; N, 14.73. Found: C, 63.27; H, 5.22; N, 14.85. ^{1}H NMR (d_6-DMSO, δ/ppm): 3.82(3H, C–H), 6.48(2H, N–H), 6.59, 6.79, 6.86, 7.02, 7.09, 7.22, 7.59(7H, C–H), 8.58(1H, C–H), 11.24(1H, O–H), 11.85 (1H, N–H). (The ^{1}H NMR spectrum of H_2L is shown in Fig. S1)

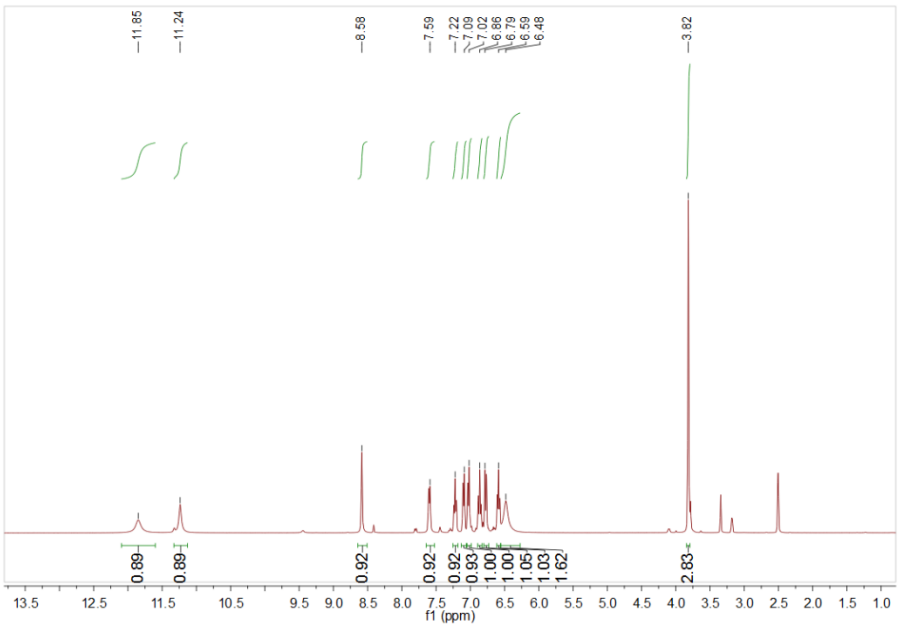

Fig. S1 ^{1}H NMR spectrum (400 MHz, d_6-DMSO) of H_2L.

Section S2 Powder X-ray Diffraction, UV-Vis spectra, Thermogravimetric Analysis and Near-infrared luminescence spectra

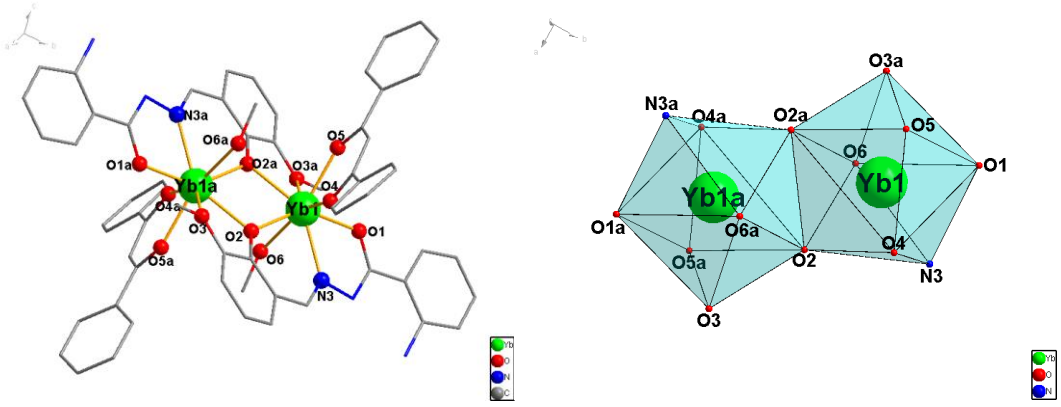

(a) (b)

Fig. S2 (a) Molecular structure of **6** (all hydrogen atoms and solvent molecules have been omitted for clarity); (b) Coordination polyhedrons for the Yb^{III} ions in complex **6**.

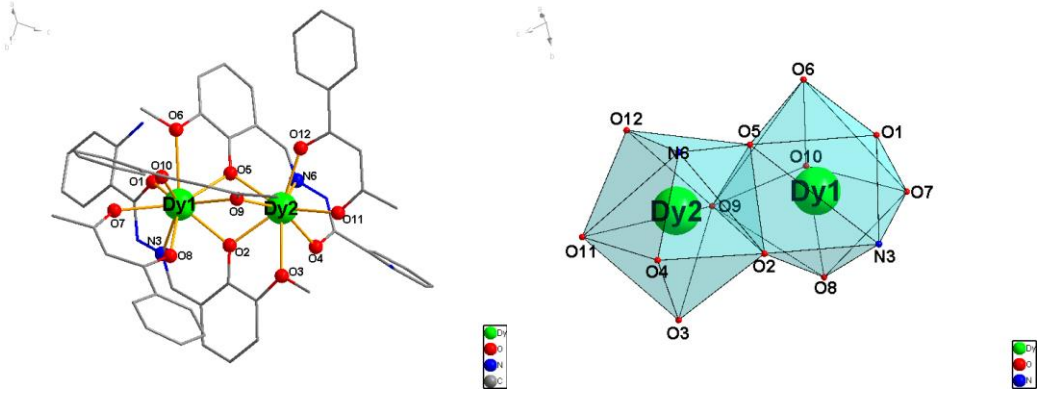

(a) (b)

Fig. S3 (a) Molecular structure of **7** (all hydrogen atoms have been omitted for clarity); (b) Coordination polyhedrons for the Dy^{III} ions in complex **7**.

Powder X-ray diffraction (PXRD)

The purity of crystalline powders of complexes **1**–**7** was confirmed by powder X-ray diffraction (PXRD), which is shown in Fig. S4 in the ESI.† The experimental patterns of **1**–**7** are in accord with the corresponding simulated patterns derived from the single crystal data, indicating the presence of mainly one crystalline phase.

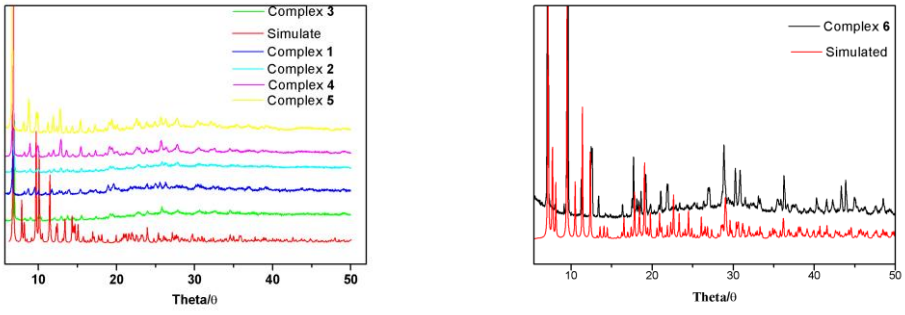

(a) (b)

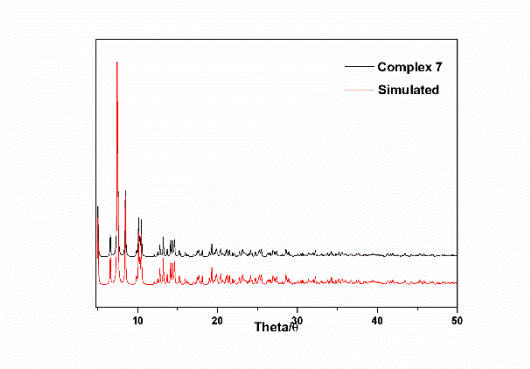

(c)

Fig. S4 PXRD patterns of complexes **1**–**5** (a), **6** (b), **7** (c).

Thermogravimetric Analysis

To confirm the thermal stability of complexes 1–**7**, TGA was performed on crystalline samples under an air atmosphere with a heating rate of 10 °C/min^{-1} in the temperature range of 30–800 °C. (Fig. S5, ESI†) Different from complex **6**, complexes **1**–**5** and **7** displayed a more stable thermogravimetric curve below 220 °C. The difference between **1**–**7** is mainly due to the discrepancies in the type and number of free solvent molecules and coordinated solvent molecules.

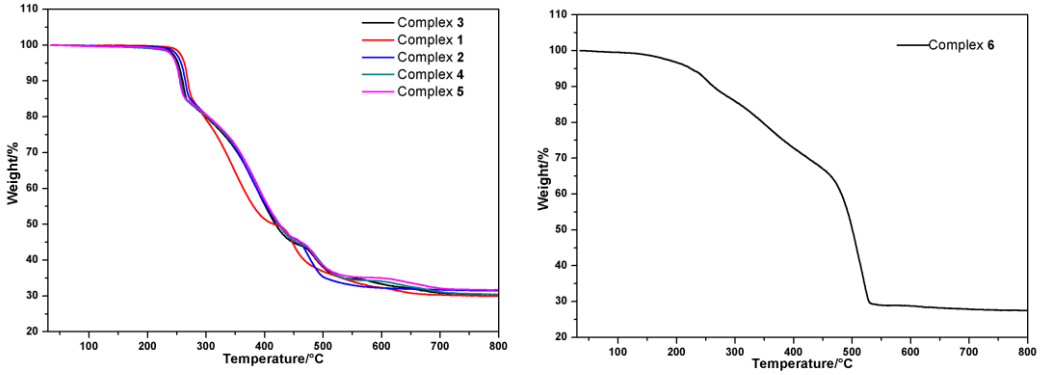

(a) (b)

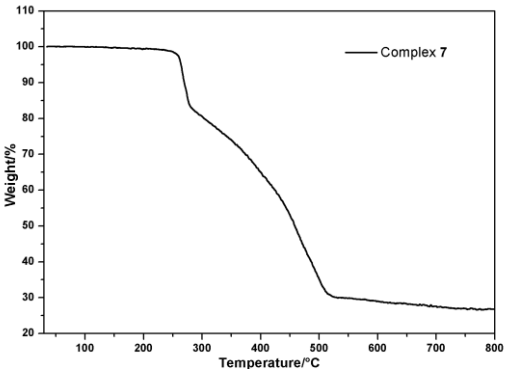

(c)

Fig. S5 TGA curves of complexes **1**–**5** (a), **6** (b), **7** (c).

UV-Vis spectra

The UV-Vis absorption spectra of $Dy(acac)_3 \cdot 2H_2O$, $Dy(dbm)_3 \cdot 2H_2O$, the ligand H_2L and the complexes **1**–**7** in dichloromethane solutions (c = 1 * 10^{-5} mol/L) were measured in the range of 200–600 nm at room temperature (Fig. S6, ESI†).

As shown in Fig. S6(a), for $Dy(acac)_3 \cdot 2H_2O$, there appears a very intense absorption band centered at ca. 287 nm and a slight shoulder peak around *ca*. 224 nm, which arise from the $\pi \rightarrow \pi^*$ transition of carbonyl from $acac^-$. The ligand H_2L shows three very intense absorption bands centered at *ca*. 233, 302 and 350 nm, which are due to the $\pi \rightarrow \pi^*$ transition of aromatic rings and the $\pi \rightarrow \pi^*$ and $n \rightarrow \pi^*$ transitions of conjugated carbonyl. Five complexes exhibit three analogous series of absorption bands centered at *ca*. 236, 292 and 378 nm. Compared to the characteristic absorption peak of ligand, for complexes, the absorption peaks of low energy bands display a red shift, which may be assigned to the coordination effect between H_2L and the Ln^{3+}.

As shown in Fig. S6(b), the $Dy(dbm)_3 \cdot 2H_2O$ has two absorption bands centered at *ca*. 254 and 345 nm, which are ascribed to the $n \rightarrow \pi^*$ and $\pi \rightarrow \pi^*$ transitions of dbm^-. The complex **6** shows two very intense absorption bands centered at *ca*. 239 and 355 nm and a slight shoulder peak around *ca*. 319 nm, respectively. In addition, it's worth noting that the band at 302 nm disappeared, which may due to the interaction between the ligand and RE^{III} ions.

In $Dy(beac)_3 \cdot 2H_2O$, two absorption bands are displayed centered at *ca*. 247 and 325 nm, respectively(Fig. S6(c), ESI†). For **7**, three absorption bands at *ca*. 242 and 309 nm and one slight shoulder peak at *ca*. 381 nm can be observed, which display a red shift relative to that of the free H_2L. This phenomenon may be assigned to the coordination effect between H_2L and the Dy^{3+} ions.

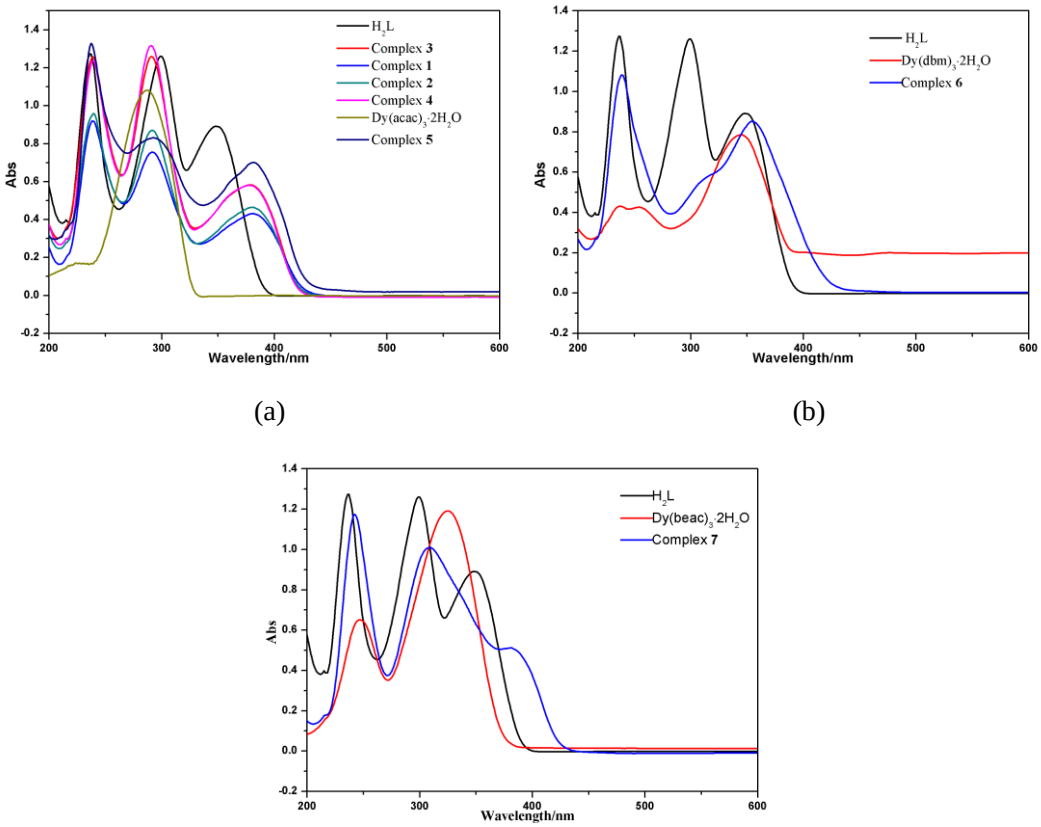

(a) (b)

(c)

Fig. S6 The UV-vis absorption spectra of $Dy(acac)_3 \cdot 2H_2O$, $Dy(dbm)_3 \cdot 2H_2O$, $Dy(beac)_3 \cdot 2H_2O$, the ligand H_2L and complexes **1–7**.

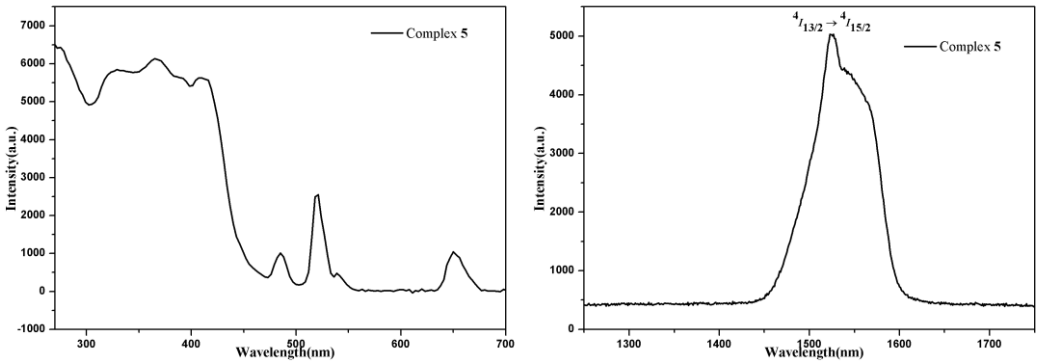

(a) (b)

Fig. S7 (a) Excitation spectrum (λ_{em} = 1523 nm) and (b) emission spectrum of complex **5** (λ_{ex} = 365 nm) in the solid state.

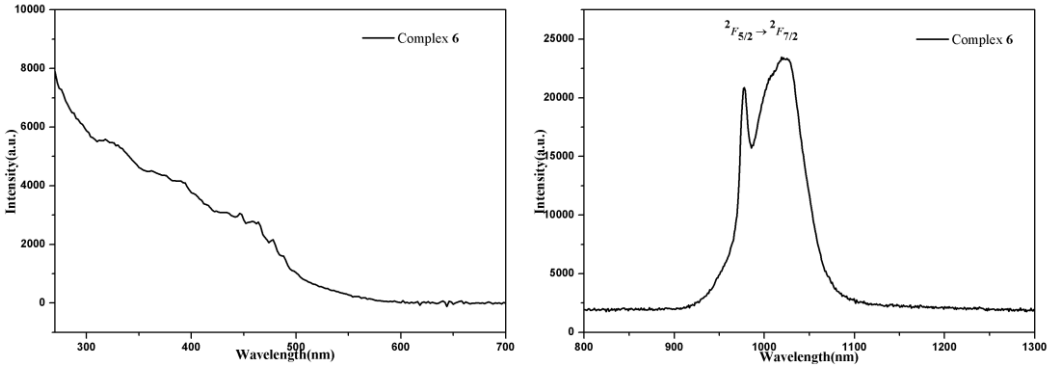

(a) (b)

Fig. S8 (a) Excitation spectrum (λ_{em} = 975 nm) and (b) emission spectrum of complex **6** (λ_{ex} = 318 nm) in the solid state.

Section S3 Plots of Magnetic Data

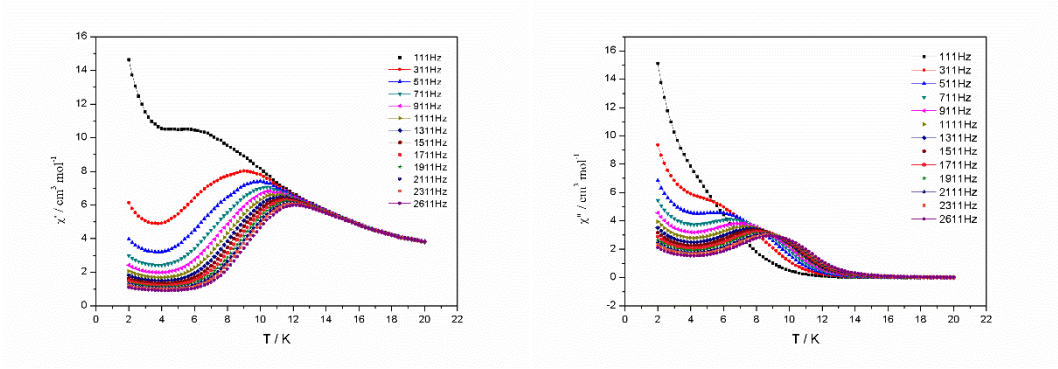

(a) (b)

Fig. S9 Plots of the temperature-dependent in-phase (a) and out-of-phase (b) *ac* susceptibility of **3**, in a zero static field and an oscillating field of 3 Oe.

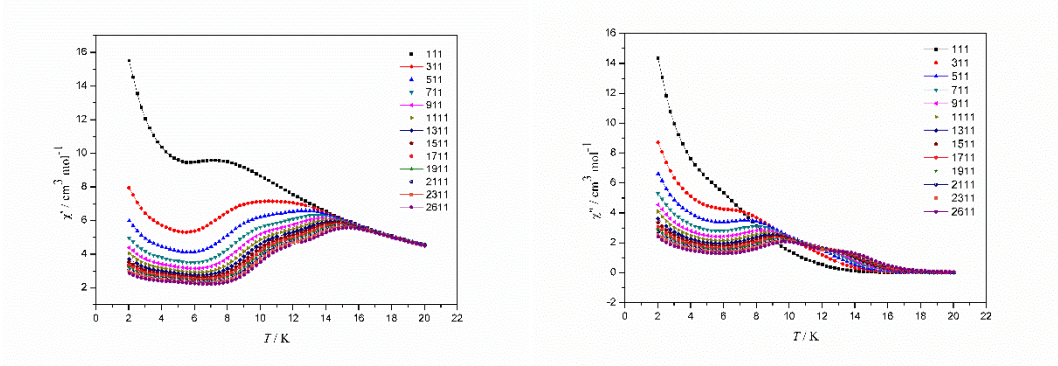

(a) (b)

Fig. S10 Plots of the temperature-dependent in-phase (a) and out-of-phase (b) *ac* susceptibility of **7**, in a zero static field and an oscillating field of 3 Oe.

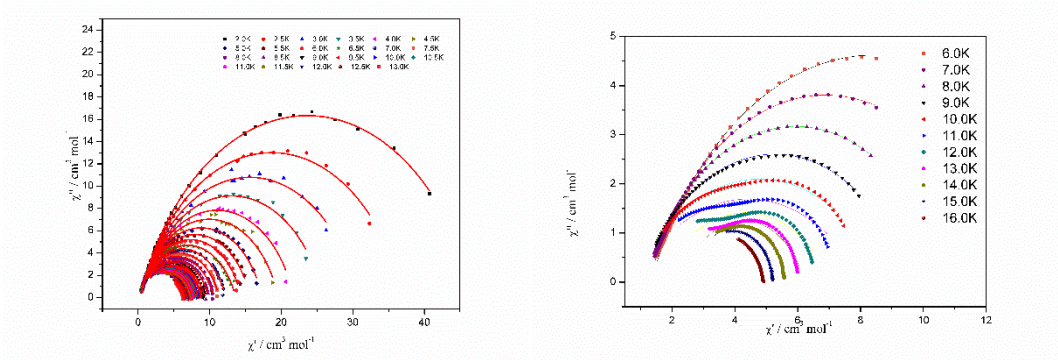

(a) (b)

Fig. S11 The Cole–Cole diagram of complexes **3** (a) and **7** (b) with solid lines as Debye fits.

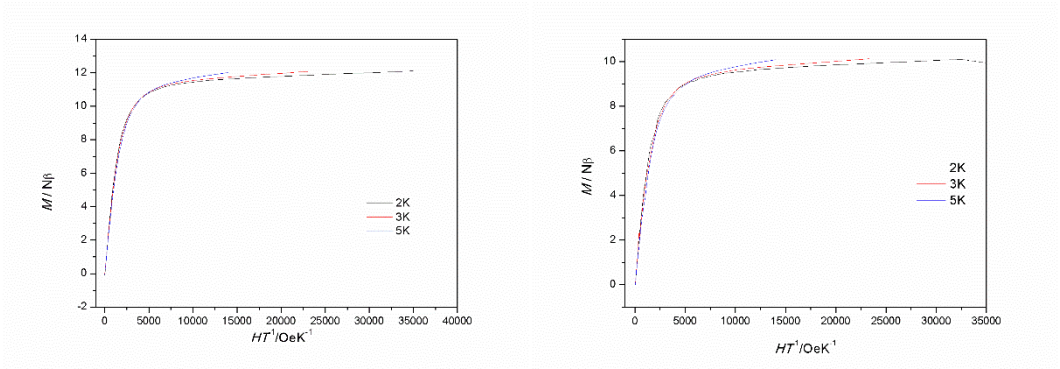

(a) (b)

Fig. S12 Plots of M vs H/T for **3** (a) and **7** (b) in the field range 0−50 kOe.

Section S4 Crystallographic Data and Continuous Shape Measures Values

Table S1 Crystal data and structure refinement for complexes **1**–**4**

Complex	**1**	**2**	**3**	**4**
Formula	$C_{51}H_{66}N_6O_{15}Eu_2$	$C_{51}H_{66}N_6O_{15}Tb_2$	$C_{51}H_{66}N_6O_{15}Dy_2$	$C_{51}H_{66}N_6O_{15}Ho_2$
M_r(g.mol^{-1})	1307.01	1320.93	1328.09	1332.95
Temperature(K)	113(2)	113(2)	113(2)	113(2)
Wavelength(Å)	0.71073	0.71073	0.71073	0.71073
Crystal system	Triclinic	Triclinic	Triclinic	Triclinic
Space group	*P*$\bar{1}$	*P*$\bar{1}$	*P*$\bar{1}$	*P*$\bar{1}$
a(Å)	13.616(3)	13.596(3)	13.630(3)	13.588(3)
b(Å)	13.689(3)	13.654(3)	13.650(3)	13.622(3)
c(Å)	17.258(4)	17.217(3)	17.230(3)	17.212(3)
α(deg)	77.36(3)	77.06(3)	76.90(3)	76.83(3)
β(deg）	68.98(3)	68.79(3)	68.64(3)	68.94(3)
γ(deg)	77.19(3)	77.60(3)	77.65(3)	77.97(3)
Volume(Å3)	2893.2(12)	2872.3(12)	2877.2(12)	2866.7(12)
Z	2	2	2	2
Calculated density(Mg m^{-3})	1.5	1.527	1.533	1.544
Abs coeff(mm^{-1})	2.214	2.509	2.644	2.807
F(000)	1320	1328	1332	1336
Crystal size(mm^3)	0.200x0.180x0.120	0.200x0.180x0.120	0.200x0.180x0.120	0.200x0.180x0.120
θ range(°)	1.622 to 25.019	1.547 to 25.020	1.286 to 25.020	1.622 to 27.873
Limiting indices	–16<=*h*<=16	–16<=*h*<=15	–16<=*h*<=16	–17<=*h*<=17
	–16<=*k*<=16	–16<=*k*<=16	–16<=*k*<=16	–17<=*k*<=17
	–20<=*l*<=20	–20<=*l*<=20	–20<=*l*<=20	–22<=*l*<=22
Reflections collected	27614	27560	26875	34518
Independent reflection	10206	10124	10129	13584
Rint	0.0351	0.0446	0.0609	0.0394
Completeness	99.90%	99.90%	99.70%	99.80%
Max.and min. transmission	1 and 0.8235	1 and 0.6803	1 and 0.8263	1 and 0.8152
Data/restraints/parameters	10206 / 37 / 684	10124 / 37 / 684	10129 / 37 / 684	13584 / 37 / 684
GoF on F^2	1.066	1.089	1.071	1.059
Final *R* indices[$I>2\sigma(I)$]	R_1 = 0.0312,	R_1 = 0.0352,	R_1 = 0.0614,	R_1 = 0.0366,
	wR_2 = 0.0789	wR_2 = 0.0877	wR_2 = 0.1560	wR_2 = 0.0838
R indices (all data)	R_1 = 0.0364,	R_1 = 0.0413,	R_1 = 0.0796,	R_1 = 0.0451,
	wR_2 = 0.0828	wR_2 = 0.0924	wR_2 = 0.1773	wR_2 = 0.0889
Largest diff.peak and hole(eÅ^{-3})	1.143 and –1.040	1.536 and –1.335	2.177 and –1.784	1.741 and –1.776

[a] $R_1 = \sum(||F_o|-|F_c||)/\sum|F_o|$. [b] $wR_2 = [\sum w(|F_o|^2-|F_c|^2)^2/\sum w(F_o^2)^2]^{1/2}$

Table S2 Crystal data and structure refinement for complexes **5**–**7**

Complex	**5**	**6**	**7**
Formula	$C_{51}H_{66}N_6O_{15}Er_2$	$C_{64}H_{64}N_6O_{14}Yb_2$	$C_{60}H_{54}N_6O_{12}Dy_2$
M_r(g.mol^{-1})	1337.61	1487.29	1376.09
Temperature(K)	113(2)	113(2)	113(2)
Wavelength(Å)	0.71073	0.71073	0.71073
Crystal system	Triclinic	Monoclinic	Monoclinic
Space group	$P\bar{1}$	$P2_1/c$	$P2_1/c$
a(Å)	13.615(3)	12.443(3)	18.959(4)
b(Å)	13.616(3)	23.026(5)	20.834(4)
c(Å)	17.183(3)	10.237(2)	15.622(3)
α(deg)	76.68(3)	90	90
β(deg)	68.59(3)	95.31(3)	113.06(3)
γ(deg)	78.05(3)	90	90
Volume(Å^3)	2859.3(12)	2920.5(10)	5677(2)
Z	2	2	4
Calculated density(Mg m^{-3})	1.554	1.691	1.61
Abs coeff(mm)	2.982	3.256	2.68
F(000)	1340	1484	2736
Crystal size(mm^3)	0.200x0.180x0.120	0.200x0.180x0.120	0.200x0.180x0.120
θ range(°)	1.292 to 25.020	1.867 to 25.017	1.523 to 25.018
Limiting indices	–16<=h<=16	–14<=h<=14	–22<=h<=22
	–15<=k<=16	–26<=k<=27	–22<=k<=24
	–20<=l<=20	–12<=l<=12	–18<=l<=18
Reflections collected	27690	20541	44791
Independent reflection	10073	5120	10015
R_{int}	0.0418	0.0787	0.0663
Completeness	99.80%	99.50%	100.00%
Max.and min. transmission	1 and 0.8611	1 and 0.4163	1 and 0.7962
Data/restraints/parameters	10073 / 37 / 684	5120 / 2 / 397	10015 / 72 / 726
GoF on F^2	0.96	1.034	1.06
Final R indices[I>2σ(I)]	R_1 = 0.0298,	R_1 = 0.0401,	R_1 = 0.0558,
	wR_2 = 0.0795	wR_2 = 0.0977	wR_2 = 0.1342
R indices (all data)	R_1 = 0.0370,	R_1 = 0.0492,	R_1 = 0.0697,
	wR_2 = 0.0945	wR_2 = 0.1039	wR_2 = 0.1449
Largest diff.peak and hole(eÅ^{-3})	1.351 and –1.180	1.805 and –1.627	1.593 and –1.784

[a] $R_1 = \sum(||F_o|-|F_c||)/\sum|F_o|$. [b] $wR_2 = [\sum w(|F_o|^2-|F_c|^2)^2/\sum w(F_o^2)^2]^{1/2}$

Table S3 The important bond lengths (Å) and angles (°) for **1**–**7**

Complexes	The range of Ln–O bond lengths / Å	The distance of Ln⋯Ln / Å	The range of Ln–O–Ln bond angles / °
1	2.345(2)-2.538(2)	3.6506(11)	93.73(8)-101.14(8)
2	2.323(3)-2.527(3)	3.6128(11)	93.72(9)-101.44(10)
3	2.304(5)-2.531(6)	3.5984(12)	93.6(2)-101.6(2)
4	2.296(2)-2.502(3)	3.5896(11)	93.48(9)-101.78(9)
5	2.284(3)-2.510(3)	3.5681(11)	93.38(10)-101.63(11)
6	2.204(4)-2.505(4)	3.6889(7)	107.18(13)
7	2.278(5)- 2.646(5)	3.6109(9)	92.85(18)-102.50(18)

Table S4 The continuous symmetry measurement value calculated by SHAPE 2.0 for complexes

Complex	Ln^{3+}	D_{4d}SAPR	D_{2d}TDD	C_{2v}JBTPR	C_{2v}BTPR
1	Eu1	3.721	**2.49**	3.995	3.422
2	Tb1	3.425	**2.315**	3.743	3.411
3	Dy2	3.337	**2.28**	3.657	3.43
4	Ho1	3.158	**2.307**	3.634	3.45
5	Er1	3.064	**2.216**	3.448	3.284
6	Yb	2.375	**0.831**	1.859	1.634
7	Dy2	3.963	**2.135**	3.412	2.992

Complex	Ln^{3+}	C_{4v}JCSAPR	C_{4v}CSAPR	D_{3h}TCTPR	C_sMFF
1	Eu2	3.103	1.693	2.612	**1.036**
2	Tb2	3.029	1.591	2.494	**0.966**
3	Dy1	3.041	1.597	2.466	**0.967**
4	Ho2	2.915	1.504	2.396	**0.895**
5	Er2	2.941	1.502	2.363	**0.909**
7	Dy1	3.221	1.653	2.345	**0.961**

Table S5 The selected bond lengths (Å) and angles (°) for **3**

Dy(1)-O(12)	2.286(6)	Dy(2)-O(8)	2.281(6)
Dy(1)-O(11)	2.295(6)	Dy(2)-O(7)	2.300(6)
Dy(1)-O(2)	2.304(5)	Dy(2)-O(2)	2.339(6)
Dy(1)-O(1)	2.316(5)	Dy(2)-O(9)	2.352(6)
Dy(1)-O(5)	2.320(5)	Dy(2)-O(5)	2.390(6)
Dy(1)-O(10)	2.403(6)	Dy(2)-O(4)	2.440(6)
Dy(1)-N(3)	2.492(7)	Dy(2)-O(10)	2.531(6)
Dy(1)-O(6)	2.591(6)	Dy(2)-O(3)	2.575(6)
Dy(1)-Dy(2)	3.5984(12)	Dy(2)-N(6)	2.576(7)
O(12)-Dy(1)-O(11)	73.0(2)	O(8)-Dy(2)-O(7)	75.4(2)
O(12)-Dy(1)-O(2)	74.9(2)	O(8)-Dy(2)-O(2)	140.9(2)
O(11)-Dy(1)-O(2)	147.9(2)	O(7)-Dy(2)-O(2)	143.6(2)
O(12)-Dy(1)-O(1)	126.2(2)	O(8)-Dy(2)-O(9)	79.2(2)

O(11)-Dy(1)-O(1)	80.1(2)	O(7)-Dy(2)-O(9)	72.1(2)
O(2)-Dy(1)-O(1)	119.9(2)	O(2)-Dy(2)-O(9)	110.9(2)
O(12)-Dy(1)-O(5)	139.7(2)	O(8)-Dy(2)-O(5)	78.4(2)
O(11)-Dy(1)-O(5)	140.6(2)	O(7)-Dy(2)-O(5)	138.0(2)
O(2)-Dy(1)-O(5)	69.2(2)	O(2)-Dy(2)-O(5)	67.47(18)
O(1)-Dy(1)-O(5)	88.23(19)	O(9)-Dy(2)-O(5)	133.5(2)
O(12)-Dy(1)-O(10)	83.4(2)	O(8)-Dy(2)-O(4)	130.1(2)
O(11)-Dy(1)-O(10)	103.8(2)	O(7)-Dy(2)-O(4)	70.5(2)
O(2)-Dy(1)-O(10)	72.5(2)	O(2)-Dy(2)-O(4)	78.38(19)
O(1)-Dy(1)-O(10)	149.0(2)	O(9)-Dy(2)-O(4)	121.2(2)
O(5)-Dy(1)-O(10)	69.04(19)	O(5)-Dy(2)-O(4)	104.31(18)
O(12)-Dy(1)-N(3)	76.9(2)	O(8)-Dy(2)-O(10)	79.6(2)
O(11)-Dy(1)-N(3)	102.3(2)	O(7)-Dy(2)-O(10)	137.9(2)
O(2)-Dy(1)-N(3)	69.9(2)	O(2)-Dy(2)-O(10)	69.59(19)
O(1)-Dy(1)-N(3)	64.4(2)	O(9)-Dy(2)-O(10)	70.4(2)
O(5)-Dy(1)-N(3)	106.3(2)	O(5)-Dy(2)-O(10)	65.85(18)
O(10)-Dy(1)-N(3)	140.9(2)	O(4)-Dy(2)-O(10)	147.87(19)
O(12)-Dy(1)-O(6)	140.6(2)	O(8)-Dy(2)-O(3)	145.4(2)
O(11)-Dy(1)-O(6)	76.3(2)	O(7)-Dy(2)-O(3)	86.1(2)
O(2)-Dy(1)-O(6)	132.02(19)	O(2)-Dy(2)-O(3)	64.03(19)
O(1)-Dy(1)-O(6)	70.60(19)	O(9)-Dy(2)-O(3)	67.3(2)
O(5)-Dy(1)-O(6)	64.31(18)	O(5)-Dy(2)-O(3)	131.50(19)
O(10)-Dy(1)-O(6)	80.4(2)	O(4)-Dy(2)-O(3)	66.6(2)
N(3)-Dy(1)-O(6)	134.4(2)	O(10)-Dy(2)-O(3)	96.2(2)
O(12)-Dy(1)-Dy(2)	98.98(17)	O(8)-Dy(2)-N(6)	76.0(2)
O(11)-Dy(1)-Dy(2)	148.42(17)	O(7)-Dy(2)-N(6)	76.6(2)
O(2)-Dy(1)-Dy(2)	39.54(15)	O(2)-Dy(2)-N(6)	104.9(2)
O(1)-Dy(1)-Dy(2)	125.62(14)	O(9)-Dy(2)-N(6)	143.9(2)
O(5)-Dy(1)-Dy(2)	40.90(14)	O(5)-Dy(2)-N(6)	65.5(2)
O(10)-Dy(1)-Dy(2)	44.59(14)	O(4)-Dy(2)-N(6)	61.6(2)
N(3)-Dy(1)-Dy(2)	105.54(16)	O(10)-Dy(2)-N(6)	128.7(2)
O(6)-Dy(1)-Dy(2)	94.26(13)	O(3)-Dy(2)-N(6)	128.2(2)
Dy(1)-O(2)-Dy(2)	101.6(2)	Dy(1)-O(5)-Dy(2)	99.64(19)
Dy(1)-O(10)-Dy(2)	93.6(2)		

Table S6 The selected bond lengths (Å) and angles (°) for **6**

Yb(1)-O(1)	2.204(4)	Yb(1)-O(4)	2.248(4)
Yb(1)-O(5)	2.258(4)	Yb(1)-O(2)	2.273(3)
Yb(1)-O(2)#1	2.310(4)	Yb(1)-O(6)	2.415(4)
Yb(1)-N(3)	2.418(4)	Yb(1)-O(3)#1	2.505(4)
Yb(1)-Yb(1)#1	3.6889(7)		
O(1)-Yb(1)-O(4)	99.06(16)	O(1)-Yb(1)-O(5)	82.32(13)
O(4)-Yb(1)-O(5)	74.33(13)	O(1)-Yb(1)-O(2)	142.04(13)
O(4)-Yb(1)-O(2)	76.55(13)	O(5)-Yb(1)-O(2)	130.21(14)

O(1)-Yb(1)-O(2)#1	140.44(13)	O(4)-Yb(1)-O(2)#1	109.95(14)
O(5)-Yb(1)-O(2)#1	80.39(12)	O(2)-Yb(1)-O(2)#1	72.82(13)
O(1)-Yb(1)-O(6)	89.60(14)	O(4)-Yb(1)-O(6)	146.59(13)
O(5)-Yb(1)-O(6)	139.03(14)	O(2)-Yb(1)-O(6)	76.93(13)
O(2)#1-Yb(1)-O(6)	80.86(14)	O(1)-Yb(1)-N(3)	66.22(14)
O(4)-Yb(1)-N(3)	79.64(15)	O(5)-Yb(1)-N(3)	135.02(13)
O(2)-Yb(1)-N(3)	75.97(14)	O(2)#1-Yb(1)-N(3)	143.76(13)
O(6)-Yb(1)-N(3)	74.50(15)	O(1)-Yb(1)-O(3)#1	75.41(14)
O(4)-Yb(1)-O(3)#1	145.88(12)	O(5)-Yb(1)-O(3)#1	71.57(12)
O(2)-Yb(1)-O(3)#1	128.13(13)	O(2)#1-Yb(1)-O(3)#1	65.43(12)
O(6)-Yb(1)-O(3)#1	67.53(13)	N(3)-Yb(1)-O(3)#1	125.27(14)

Table S7 The selected bond lengths (Å) and angles (°) for **7**

Dy(1)-O(8)	2.278(5)	Dy(2)-O(2)	2.287(5)
Dy(1)-O(7)	2.326(5)	Dy(2)-O(12)	2.291(5)
Dy(1)-O(2)	2.365(5)	Dy(2)-O(4)	2.308(5)
Dy(1)-O(9)	2.580(6)	Dy(2)-O(11)	2.309(5)
Dy(1)-O(6)	2.646(5)	Dy(2)-O(5)	2.312(5)
Dy(1)-O(5)	2.318(5)	Dy(2)-O(9)	2.401(5)
Dy(1)-O(10)	2.334(6)	Dy(2)-N(6)	2.488(6)
Dy(1)-O(1)	2.393(5)	Dy(2)-O(3)	2.619(5)
Dy(1)-N(3)	2.618(6)		
O(8)-Dy(1)-O(5)	137.12(17)	O(9)-Dy(1)-O(6)	89.16(18)
O(5)-Dy(1)-O(7)	148.51(18)	N(3)-Dy(1)-O(6)	128.44(17)
O(8)-Dy(1)-O(7)	74.27(19)	O(2)-Dy(2)-O(12)	144.06(19)
O(8)-Dy(1)-O(10)	77.7(2)	O(2)-Dy(2)-O(4)	88.53(17)
O(5)-Dy(1)-O(10)	111.5(2)	O(12)-Dy(2)-O(4)	122.21(19)
O(7)-Dy(1)-O(10)	72.1(2)	O(2)-Dy(2)-O(11)	137.5(2)
O(8)-Dy(1)-O(2)	76.61(16)	O(12)-Dy(2)-O(11)	72.3(2)
O(5)-Dy(1)-O(2)	66.66(16)	O(4)-Dy(2)-O(11)	78.7(2)
O(7)-Dy(1)-O(2)	135.28(19)	O(2)-Dy(2)-O(5)	68.03(17)
O(10)-Dy(1)-O(2)	132.5(2)	O(12)-Dy(2)-O(5)	79.18(19)
O(8)-Dy(1)-O(1)	135.29(18)	O(4)-Dy(2)-O(5)	121.66(18)
O(5)-Dy(1)-O(1)	78.17(17)	O(11)-Dy(2)-O(5)	151.2(2)
O(7)-Dy(1)-O(1)	73.72(18)	O(2)-Dy(2)-O(9)	71.59(18)
O(10)-Dy(1)-O(1)	119.9(2)	O(12)-Dy(2)-O(9)	84.0(2)
O(2)-Dy(1)-O(1)	106.46(17)	O(4)-Dy(2)-O(9)	151.72(18)
O(8)-Dy(1)-O(9)	79.37(18)	O(11)-Dy(2)-O(9)	102.2(2)
O(5)-Dy(1)-O(9)	66.76(17)	O(5)-Dy(2)-O(9)	69.99(19)
O(7)-Dy(1)-O(9)	136.79(18)	O(2)-Dy(2)-N(6)	104.01(19)
O(10)-Dy(1)-O(9)	69.2(2)	O(12)-Dy(2)-N(6)	77.1(2)
O(2)-Dy(1)-O(9)	67.23(17)	O(4)-Dy(2)-N(6)	64.83(18)
O(1)-Dy(1)-O(9)	144.05(17)	O(11)-Dy(2)-N(6)	106.6(2)
O(8)-Dy(1)-N(3)	81.43(18)	O(5)-Dy(2)-N(6)	70.30(18)

O(5)-Dy(1)-N(3)	101.79(17)	O(9)-Dy(2)-N(6)	138.4(2)
O(7)-Dy(1)-N(3)	77.00(19)	O(2)-Dy(2)-O(3)	63.26(16)
O(10)-Dy(1)-N(3)	146.3(2)	O(12)-Dy(2)-O(3)	138.79(18)
O(2)-Dy(1)-N(3)	65.65(17)	O(4)-Dy(2)-O(3)	72.77(16)
O(1)-Dy(1)-N(3)	61.53(17)	O(11)-Dy(2)-O(3)	74.2(2)
O(9)-Dy(1)-N(3)	131.98(17)	O(5)-Dy(2)-O(3)	128.71(16)
O(8)-Dy(1)-O(6)	144.73(17)	O(9)-Dy(2)-O(3)	80.24(18)
O(5)-Dy(1)-O(6)	62.66(16)	N(6)-Dy(2)-O(3)	136.17(18)
O(7)-Dy(1)-O(6)	93.03(18)	Dy(2)-O(5)-Dy(1)	102.50(18)
O(10)-Dy(1)-O(6)	67.10(19)	Dy(2)-O(9)-Dy(1)	92.85(18)
O(2)-Dy(1)-O(6)	129.16(16)	Dy(2)-O(2)-Dy(1)	101.82(19)
O(1)-Dy(1)-O(6)	67.09(17)		

Table S8 Relaxation fitting parameters for Cole–Cole plots of **3** at varying temperatures under zero applied *dc*-field using the Debye model of a single relaxation process.

T/K	χ_S	χ_T	α
2	0.324566	46.6595	0.21231
2.5	0.284723	37.231	0.21616
3	0.276126	30.8439	0.217435
3.5	0.313524	26.061	0.210281
4	0.317351	22.1125	0.202347
4.5	0.291704	19.8257	0.203137
5	0.255163	17.4893	0.200439
5.5	0.234004	15.6669	0.194274
6	0.18813	14.4749	0.199761
6.5	0.128593	13.4407	0.209132
7	0.119789	12.2373	0.203843
7.5	0.0829678	11.3554	0.210192
8	0.0395865	10.6392	0.223372
8.5	0.0352615	9.95583	0.235701
9	0.0727222	9.40711	0.249701
9.5	0.233394	8.88272	0.249989
10	0.450528	8.41784	0.24499
10.5	0.752454	7.95388	0.226193
11	0.986109	7.54929	0.214235
11.5	1.1975	7.18481	0.205233
12	1.23901	6.87066	0.21118
12.5	1.43463	6.55247	0.202614
13	1.20546	6.31102	0.237163

Table S9 Relaxation fitting parameters for Cole-Cole plots of **7** at varying temperatures under 1500 Oe applied *dc*-field using the Debye model of a single relaxation process

T/K	χ_S	χ_T	α
6	1.33003	15.4881	0.263164
7	1.27279	12.5089	0.240634
8	1.15549	10.7113	0.253124
9	0.982641	9.57579	0.305355
10	0.773179	8.79965	0.386028
11	0.788521	8.07616	0.445951
12	1.57009	7.09293	0.397179
13	2.31869	6.23814	0.275362
14	2.60084	5.65393	0.180343
15	2.67224	5.23521	0.130386
16	2.66929	4.90795	0.125521

Table S10 Standard error for the extracted magnetic parameters

	Value for **3** in zero *dc* field	Standard error for **3** in zero *dc* field	Value for **7** in 1500 Oe *dc* field	Standard error for **7** in 1500 Oe *dc* field
τ_0	$1.29941*10^{-10}$	$7.75495*10^{-11}$	$2.6663*10^{-7}$	$1.66056*10^{-7}$
U_{eff}	140.38181	7.45835	75.19653	11.16601
C	0.69685	0.16516	3.54292	0.58483
n	4.19909	0.12633	2.87686	0.71363
A	1	0	0	0
m	-10	0	1	0
τ_{QTM}	0.00276	0	105	0